Pergamon

Int. J. Solids Structures Vol. 31, No. 21, pp. 2965–2977, 1994

0020–7683/94 $7.00 + .00

0020–7683(94)E0062–Z

CHARACTERIZATION OF A HORIZONTAL CRACK IN ANISOTROPIC LAMINATED PLATES

G. R. LIU and K. Y. LAM
Department of Mechanical and Production Engineering, National University of Singapore, 10 Kent Ridge Crescent, Singapore 0511

(*Received* 2 *October* 1993; *in revised form* 12 *April* 1994)

Abstract—A technique is presented for the characterization of a horizontal crack in an anisotropic laminated plate. In this technique, a distributed harmonic load is applied on the plate surface and then moved along the plate surface. The displacement in the thickness direction of the plate at the central point of the distributed load is computed by using the strip element method. The crack length is approximately determined from pattern change of the responses, which is found to have significant change when the load moves over the crack tips. The crack depth is determined from the intervals of the oscillations of the responses in the region between the two crack tips; the intervals are found to be dependent on the crack depth and less dependent on the crack length. Approximate polynomial formulae of degree three for predicting the depths of horizontal cracks in isotropic homogeneous and anisotropic laminated plates are also proposed.

1. INTRODUCTION

Ultrasonic techniques play a very important role in detecting cracks in materials. Cracks in composite laminated plates can also be detected and characterized by ultrasonic techniques, even though reliable results are much more difficult to obtain than for materials, such as metals, that are homogeneous to a much smaller scale. In fiber reinforced composites, the individual fibers are micrometers in diameter and the thicknesses of plies are of the order of one-tenth of a millimetre. It would not be productive to attempt detection of cracks with signals whose dominant wavelength is one-tenth of a millimetre or less. Such signals would generate too much interference with the inhomogeneity of the material and they would be rapidly attenuated. Lower frequency signals whose dominant wavelength is of the order of the thickness of laminated plates, say millimetres, will propagate over longer distances, since less interference is generated by such lower frequency signals. On the other hand, however, the lower the frequency of the input signal, the less sensitive it is to the cracks. Hence it would be difficult to use very low frequency signals whose dominant wavelength is much longer than the plate thickness to detect cracks whose sizes are of the order of the plate thickness.

The most important key in using the ultrasonic techniques successfully is to find out the relationships between the characteristics of a crack and the scattered ultrasonic wave fields. However, the finding of the relationships is very difficult. Basically the problem for finding the relationship is usually an inverse problem, which needs a lot of computational efforts. To solve an inverse problem, a large number of corresponding forward problems has to be solved. Hence a very efficient method and suitable modeling for solving the forward problem are a necessary prerequisite.

Scattering of waves in an elastic layer has been investigated by Al-Nassar *et al.* (1991) and Karunasena *et al.* (1991) by using a combined finite element and Lamb wave modal expansion method. Dispersion equations for Lamb waves were obtained by an exact method. Karim *et al.* (1992) presented a similar technique which combines the finite element method and guided wave mode expansions to calculate scattering of Lamb waves by cracks or inclusions. In this method the finite element boundary has to be far away from the loads and inclusions, because only Lamb waves with real wave numbers have been used in the exterior regions. The boundary element method (BEM) has also been used for investigating scattered waves in a half space and finite depth strata (Von Estorff *et al.*, 1990), where a semi-numerical method was used to calculate Green's functions. Another efficient way,

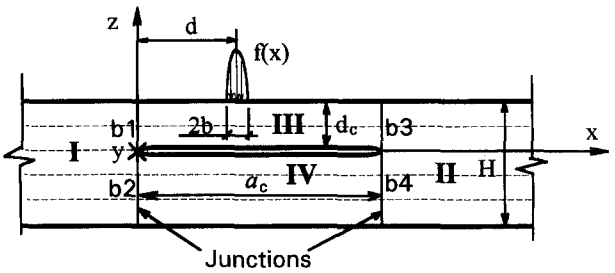

Fig. 1. Division of a plate with a horizontal crack into domains in which the SEM can be applied.

presented by Liu and Datta (1993) and Liu *et al.* (1991b), to investigate scattering of Lamb waves is to combine the BEM and FEM, where the FEM is used for the interior region and the BEM is used for the exterior region. Green's functions for the BEM were obtained by using an integration technique given by Xu and Mal (1987). A strip element method (SEM) has been proposed by Liu and Achenbach (1994a) for stress analysis of anisotropic linearly elastic solids. In the SEM, the problem domain is first divided into a set of strip elements. Then a dimension-reduced system of approximate differential equations is derived for the strip elements by using the principle of virtual work. These equations are then solved analytically. This method maintains many advantages of the FEM and BEM, but it requires much less data storage. As in the FEM, the SEM can be used for anisotropic solids, but like in the BEM, it only requires a small memory. The SEM has lately been extended to investigate the scattering of waves by cracks in anisotropic laminated plates (Liu and Achenbach, 1994b). The SEM provides a very good choice of methods for solving forward problems of wave propagation in cracked anisotropic laminated plates. The major advantage of the SEM for solving wave scattering problems is the much smaller number of equations compared with the finite element method (FEM). Consequently much shorter computing time is needed for solutions of comparable accuracy.

In this paper the SEM is used to investigate the scattering of the wave fields in plates by cracks; a technique is then presented for detecting a horizontal crack in plates. Numerical experiments are made and it is shown that both the crack length and depth of a horizontal crack in plates can be successfully detected.

2. STATEMENT OF THE PROBLEM

Consider an infinite plate containing a horizontal crack as shown in Fig. 1. The material of the plate can be isotropic or anisotropic, and inhomogeneous in the thickness direction such as in laminated composite plates. The thickness of the plate is denoted by H, the length of the horizonal crack is denoted by a_c, and the depth of the crack from the upper surface of the plate is denoted by d_c. To simplify the problem, we assume that the crack is throughout in the y-direction. The purpose of this paper is to provide a possible technique to detect the crack and determine both the length and depth of the crack, by exciting the plate with harmonic loads and analysing the subsequent responses of plate.

3. SOLUTION TO THE PROBLEM

3.1. *Load applied to the plate*

The plate is first excited by a harmonic loading which does not vary with the y-direction. Hence the problem is two-dimensional and is in the frequency domain. The load acting on the surface of the plate is given by

$$F(x) = q_0 f(x) \exp(i\omega t), \tag{1}$$

where q_0 is a constant and $f(x)$ represents the distribution of the load along the x-direction as shown in Fig. 1. In this paper, $f(x)$ is assumed as follows:

$$f(x) = \begin{cases} \exp[-\{(x+d)/\alpha\}^2], & |x-d| \leqslant b \\ 0, & |x-d| \geqslant b \end{cases} \tag{2}$$

Equation (2) is an approximation of a load generated by a laser beam, where d is the offset of the center of the load from the origin (left crack tip), and b is the half-width of the applied load, while α is a parameter which controls the distribution of the load. In this paper, b and α are chosen to be $0.1H$ and $0.05H$, respectively.

3.2. *The strip element method (SEM)*

The procedures for using the SEM to solve the (two-dimensional) problem of wave propagation in an anisotropic laminated plate are listed below.

- Divide the plate into some strip elements in the thickness direction.
- Derive an approximate governing differential equation for the field dependencies by using the principle of virtual work for each element. This governing equation, which plays the role of the equation of motion, is a one-dimension-reduced differential equation. The field dependencies are functions of time and the horizontal coordinate.
- Assemble the approximate governing differential equations for all elements; a set of approximate differential equations for the whole plate is obtained by using the boundary conditions in the horizonal direction.
- Solve the set of approximate differential equations analytically. The solution is a sum of a particular solution and the complementary solution containing unknown constants.
- Replace the unknown constants by unknown displacements on the vertical boundaries, resulting in a set of equations which gives the relationship between the displacements and stresses at the nodal points on the vertical boundaries of the domains.
- Solve the set of equations by using the vertical boundary conditions, the whole wave field can then be easily obtained.

Detailed formulations have been given in papers by Liu and Achenbach (1994a, b).

3.3. *Application of SEM to a plate with a horizontal crack*

The cracked plate is divided into four sub-domains as denoted by Roman numerals in Fig. 1. Domain I is bounded by boundaries b1, b2 and the upper and lower surfaces of the plate. Domain II is bounded by boundaries b3, b4 and the upper and lower surfaces of the plate. Domain III is bounded by boundary b1, b3, the upper surface of the plate and the upper surface of the crack. Domain IV is bounded by boundaries b2 and b4, the lower surfaces of the crack and the lower surface of the plate. In each domain the SEM is used to obtain sets of equations which gives the relationship between the displacements and stresses at the nodal points on the vertical boundaries of the sub-domains. For domain I, we can obtain (Liu and Achenbach, 1994b)

$$\mathbf{R}_b^I = \mathbf{K}_b^I + \mathbf{S}_b^I, \tag{3}$$

where the superscript of the Roman numeral indicates the domain which the equation governs, while $\mathbf{K}$ is the stiffness matrix of the domain. Vectors $\mathbf{R}$, $\mathbf{V}$ and $\mathbf{S}$ are, respectively, the external force vector acting on the vertical boundary, displacement vector on the vertical boundary, and the equivalent stress vector caused by the external force acting on the horizontal boundaries of the domain [see Liu and Achenbach (1994b)]. Equation (3) can be further divided into sub-matrices as follows:

$$\begin{Bmatrix} \mathbf{R}^{\mathrm{I}}_{\mathrm{b1}} \\ \mathbf{R}^{\mathrm{I}}_{\mathrm{bL}} \\ \mathbf{R}^{\mathrm{I}}_{\mathrm{b2}} \end{Bmatrix} = \begin{bmatrix} \mathbf{K}^{\mathrm{I}}_{11} & \mathbf{K}^{\mathrm{I}}_{12} & \mathbf{K}^{\mathrm{I}}_{13} \\ \mathbf{K}^{\mathrm{I}}_{21} & \mathbf{K}^{\mathrm{I}}_{22} & \mathbf{K}^{\mathrm{I}}_{23} \\ \mathbf{K}^{\mathrm{I}}_{31} & \mathbf{K}^{\mathrm{I}}_{32} & \mathbf{K}^{\mathrm{I}}_{33} \end{bmatrix} \begin{Bmatrix} \mathbf{V}^{\mathrm{I}}_{\mathrm{b1}} \\ \mathbf{V}^{\mathrm{I}}_{\mathrm{bL}} \\ \mathbf{V}^{\mathrm{I}}_{\mathrm{b2}} \end{Bmatrix} + \begin{Bmatrix} \mathbf{S}^{\mathrm{I}}_{\mathrm{b1}} \\ \mathbf{S}^{\mathrm{I}}_{\mathrm{bL}} \\ \mathbf{S}^{\mathrm{I}}_{\mathrm{b2}} \end{Bmatrix}, \tag{4}$$

where the subscripts b1 and b2 stand, respectively, for the vectors on the upper and lower right vertical boundary of the domain excluding the left crack tip. The subscript bL stands for the vectors at the left crack tip.

Similarly, for domain II we obtain

$$\begin{Bmatrix} \mathbf{R}^{\mathrm{II}}_{\mathrm{b3}} \\ \mathbf{R}^{\mathrm{II}}_{\mathrm{bR}} \\ \mathbf{R}^{\mathrm{II}}_{\mathrm{b4}} \end{Bmatrix} = \begin{bmatrix} \mathbf{K}^{\mathrm{II}}_{11} & \mathbf{K}^{\mathrm{II}}_{12} & \mathbf{K}^{\mathrm{II}}_{13} \\ \mathbf{K}^{\mathrm{II}}_{21} & \mathbf{K}^{\mathrm{II}}_{22} & \mathbf{K}^{\mathrm{II}}_{23} \\ \mathbf{K}^{\mathrm{II}}_{31} & \mathbf{K}^{\mathrm{II}}_{32} & \mathbf{K}^{\mathrm{II}}_{33} \end{bmatrix} \begin{Bmatrix} \mathbf{V}^{\mathrm{II}}_{\mathrm{b3}} \\ \mathbf{V}^{\mathrm{II}}_{\mathrm{bR}} \\ \mathbf{V}^{\mathrm{II}}_{\mathrm{b4}} \end{Bmatrix} + \begin{Bmatrix} \mathbf{S}^{\mathrm{II}}_{\mathrm{b3}} \\ \mathbf{S}^{\mathrm{II}}_{\mathrm{bR}} \\ \mathbf{S}^{\mathrm{II}}_{\mathrm{b4}} \end{Bmatrix}, \tag{5}$$

where the subscripts b3 and b4 stand, respectively, for the vectors on the upper and lower left vertical boundary of domain II excluding the right crack tip. The subscript bR stands for the vectors at the right crack tip. For domains III and IV, we have

$$\begin{Bmatrix} \mathbf{R}^{\mathrm{III}}_{\mathrm{b1}} \\ \mathbf{R}^{\mathrm{III}}_{\mathrm{bL}} \\ \mathbf{R}^{\mathrm{III}}_{\mathrm{b3}} \\ \mathbf{R}^{\mathrm{III}}_{\mathrm{bR}} \end{Bmatrix} = \begin{bmatrix} \mathbf{K}^{\mathrm{III}}_{11} & \mathbf{K}^{\mathrm{III}}_{12} & \mathbf{K}^{\mathrm{III}}_{13} & \mathbf{K}^{\mathrm{III}}_{14} \\ \mathbf{K}^{\mathrm{III}}_{21} & \mathbf{K}^{\mathrm{III}}_{22} & \mathbf{K}^{\mathrm{III}}_{23} & \mathbf{K}^{\mathrm{III}}_{24} \\ \mathbf{K}^{\mathrm{III}}_{31} & \mathbf{K}^{\mathrm{III}}_{32} & \mathbf{K}^{\mathrm{III}}_{33} & \mathbf{K}^{\mathrm{III}}_{34} \\ \mathbf{K}^{\mathrm{III}}_{41} & \mathbf{K}^{\mathrm{III}}_{42} & \mathbf{K}^{\mathrm{III}}_{43} & \mathbf{K}^{\mathrm{III}}_{44} \end{bmatrix} \begin{Bmatrix} \mathbf{V}^{\mathrm{III}}_{\mathrm{b1}} \\ \mathbf{V}^{\mathrm{III}}_{\mathrm{bL}} \\ \mathbf{V}^{\mathrm{III}}_{\mathrm{b3}} \\ \mathbf{V}^{\mathrm{III}}_{\mathrm{bR}} \end{Bmatrix} + \begin{Bmatrix} \mathbf{S}^{\mathrm{III}}_{\mathrm{b1}} \\ \mathbf{S}^{\mathrm{III}}_{\mathrm{bL}} \\ \mathbf{S}^{\mathrm{III}}_{\mathrm{b3}} \\ \mathbf{S}^{\mathrm{III}}_{\mathrm{bR}} \end{Bmatrix} \tag{6}$$

and

$$\begin{Bmatrix} \mathbf{R}^{\mathrm{IV}}_{\mathrm{bL}} \\ \mathbf{R}^{\mathrm{IV}}_{\mathrm{b2}} \\ \mathbf{R}^{\mathrm{IV}}_{\mathrm{bR}} \\ \mathbf{R}^{\mathrm{IV}}_{\mathrm{b4}} \end{Bmatrix} = \begin{bmatrix} \mathbf{K}^{\mathrm{IV}}_{11} & \mathbf{K}^{\mathrm{IV}}_{12} & \mathbf{K}^{\mathrm{IV}}_{13} & \mathbf{K}^{\mathrm{IV}}_{14} \\ \mathbf{K}^{\mathrm{IV}}_{21} & \mathbf{K}^{\mathrm{IV}}_{22} & \mathbf{K}^{\mathrm{IV}}_{23} & \mathbf{K}^{\mathrm{IV}}_{24} \\ \mathbf{K}^{\mathrm{IV}}_{31} & \mathbf{K}^{\mathrm{IV}}_{32} & \mathbf{K}^{\mathrm{IV}}_{33} & \mathbf{K}^{\mathrm{IV}}_{34} \\ \mathbf{K}^{\mathrm{IV}}_{41} & \mathbf{K}^{\mathrm{IV}}_{42} & \mathbf{K}^{\mathrm{IV}}_{43} & \mathbf{K}^{\mathrm{IV}}_{44} \end{bmatrix} \begin{Bmatrix} \mathbf{V}^{\mathrm{IV}}_{\mathrm{bL}} \\ \mathbf{V}^{\mathrm{IV}}_{\mathrm{b2}} \\ \mathbf{V}^{\mathrm{IV}}_{\mathrm{bR}} \\ \mathbf{V}^{\mathrm{IV}}_{\mathrm{b4}} \end{Bmatrix} + \begin{Bmatrix} \mathbf{S}^{\mathrm{IV}}_{\mathrm{bL}} \\ \mathbf{S}^{\mathrm{IV}}_{\mathrm{b2}} \\ \mathbf{S}^{\mathrm{IV}}_{\mathrm{bR}} \\ \mathbf{S}^{\mathrm{IV}}_{\mathrm{b4}} \end{Bmatrix}. \tag{7}$$

By assembling all the sets of the equations for all the domains by using the following continuity conditions at the junctions which divide the plate into sub-domains,

$$\mathbf{R}_{\mathrm{b1}} = \mathbf{R}^{\mathrm{I}}_{\mathrm{b1}} - \mathbf{R}^{\mathrm{III}}_{\mathrm{b1}}, \quad \mathbf{V}_{\mathrm{b1}} = \mathbf{V}^{\mathrm{I}}_{\mathrm{b1}} = \mathbf{V}^{\mathrm{III}}_{\mathrm{b1}} \tag{8}$$

$$\mathbf{R}_{\mathrm{bL}} = \mathbf{R}^{\mathrm{I}}_{\mathrm{bL}} - \mathbf{R}^{\mathrm{III}}_{\mathrm{bL}} - \mathbf{R}^{\mathrm{IV}}_{\mathrm{bL}}, \quad \mathbf{V}_{\mathrm{bL}} = \mathbf{V}^{\mathrm{I}}_{\mathrm{bL}} = \mathbf{V}^{\mathrm{III}}_{\mathrm{bL}} = \mathbf{V}^{\mathrm{IV}}_{\mathrm{bL}} \tag{9}$$

$$\mathbf{R}_{\mathrm{b2}} = \mathbf{R}^{\mathrm{I}}_{\mathrm{b2}} - \mathbf{R}^{\mathrm{IV}}_{\mathrm{b2}} \quad \mathbf{V}_{\mathrm{b2}} = \mathbf{V}^{\mathrm{I}}_{\mathrm{b2}} = \mathbf{V}^{\mathrm{IV}}_{\mathrm{b2}} \tag{10}$$

$$\mathbf{R}_{\mathrm{b3}} = \mathbf{R}^{\mathrm{III}}_{\mathrm{b3}} - \mathbf{R}^{\mathrm{II}}_{\mathrm{b3}}, \quad \mathbf{V}_{\mathrm{b3}} = \mathbf{V}^{\mathrm{II}}_{\mathrm{b3}} = \mathbf{V}^{\mathrm{III}}_{\mathrm{b3}} \tag{11}$$

$$\mathbf{R}_{\mathrm{bR}} = \mathbf{R}^{\mathrm{III}}_{\mathrm{bR}} + \mathbf{R}^{\mathrm{IV}}_{\mathrm{bR}} - \mathbf{R}^{\mathrm{II}}_{\mathrm{bR}}, \quad \mathbf{V}_{\mathrm{bR}} = \mathbf{V}^{\mathrm{II}}_{\mathrm{bR}} = \mathbf{V}^{\mathrm{III}}_{\mathrm{bR}} = \mathbf{V}^{\mathrm{IV}}_{\mathrm{bR}} \tag{12}$$

$$\mathbf{R}_{\mathrm{b4}} = \mathbf{R}^{\mathrm{IV}}_{\mathrm{b4}} - \mathbf{R}^{\mathrm{II}}_{\mathrm{b4}}, \quad \mathbf{V}_{\mathrm{b4}} = \mathbf{V}^{\mathrm{II}}_{\mathrm{b4}} = \mathbf{V}^{\mathrm{IV}}_{\mathrm{b4}}, \tag{13}$$

a set of equations which gives the relationship between the displacements and stresses at all nodal points on the junctions can then be obtained. The equations are

$$\mathbf{R}_{\mathrm{J}} = \mathbf{K}\mathbf{V}_{\mathrm{J}} + \mathbf{S}_{\mathrm{J}}, \tag{14}$$

where $\mathbf{R}_{\mathrm{J}}$ is the external force vector acting on the junctions given by

$$\mathbf{R}_J = \{\mathbf{R}_{b1} \quad \mathbf{R}_{bL} \quad \mathbf{R}_{b2} \quad \mathbf{R}_{b3} \quad \mathbf{R}_{bR} \quad \mathbf{R}_{b4}\}^T \tag{15}$$

and $\mathbf{V}_J$ is the displacement vector acting on the junctions as follows

$$\mathbf{V}_J = \{\mathbf{V}_{b1} \quad \mathbf{V}_{bL} \quad \mathbf{V}_{b2} \quad \mathbf{V}_{b3} \quad \mathbf{V}_{bR} \quad \mathbf{V}_{b4}\}^T. \tag{16}$$

In eqn (14), $\mathbf{S}_J$ is given by

$$\mathbf{S}_J = \begin{Bmatrix} \mathbf{S}_{b1}^{I} - \mathbf{S}_{b1}^{III} \\ \mathbf{S}_{bL}^{I} - \mathbf{S}_{bL}^{III} - \mathbf{S}_{bL}^{IV} \\ \mathbf{S}_{b2}^{I} - \mathbf{S}_{b2}^{IV} \\ -\mathbf{S}_{b3}^{II} + \mathbf{S}_{b3}^{III} \\ -\mathbf{S}_{bR}^{II} + \mathbf{S}_{bR}^{III} + \mathbf{S}_{bR}^{IV} \\ -\mathbf{S}_{b4}^{II} + \mathbf{S}_{b4}^{IV} \end{Bmatrix}. \tag{17}$$

In eqn (14), $\mathbf{K}$ is the stiffness matrix for the cracked plate given by

$$\mathbf{K} = \begin{bmatrix} \mathbf{K}_{11}^{I} - \mathbf{K}_{11}^{III} & \mathbf{K}_{12}^{I} - \mathbf{K}_{12}^{III} & \mathbf{K}_{13}^{I} & -\mathbf{K}_{13}^{III} & -\mathbf{K}_{14}^{III} & 0 \\ \mathbf{K}_{21}^{I} - \mathbf{K}_{21}^{III} & \mathbf{K}_{22}^{I} - \mathbf{K}_{22}^{III} - \mathbf{K}_{11}^{IV} & \mathbf{K}_{23}^{I} - \mathbf{K}_{12}^{IV} & -\mathbf{K}_{23}^{III} & -\mathbf{K}_{24}^{III} - \mathbf{K}_{13}^{IV} & -\mathbf{K}_{14}^{IV} \\ \mathbf{K}_{31}^{I} & \mathbf{K}_{32}^{I} - \mathbf{K}_{21}^{IV} & \mathbf{K}_{33}^{I} - \mathbf{K}_{22}^{IV} & 0 & -\mathbf{K}_{23}^{IV} & -\mathbf{K}_{24}^{IV} \\ \mathbf{K}_{31}^{III} & \mathbf{K}_{32}^{III} & 0 & \mathbf{K}_{33}^{III} - \mathbf{K}_{11}^{II} & \mathbf{K}_{34}^{III} - \mathbf{K}_{12}^{II} & -\mathbf{K}_{13}^{II} \\ \mathbf{K}_{41}^{III} & \mathbf{K}_{42}^{III} + \mathbf{K}_{31}^{IV} & \mathbf{K}_{32}^{IV} & \mathbf{K}_{43}^{III} - \mathbf{K}_{21}^{II} & \mathbf{K}_{44}^{III} - \mathbf{K}_{22}^{II} + \mathbf{K}_{33}^{IV} & \mathbf{K}_{34}^{IV} - \mathbf{K}_{23}^{II} \\ 0 & \mathbf{K}_{41}^{IV} & \mathbf{K}_{42}^{IV} & -\mathbf{K}_{31}^{II} & \mathbf{K}_{43}^{IV} - \mathbf{K}_{32}^{II} & \mathbf{K}_{44}^{IV} - \mathbf{K}_{33}^{II} \end{bmatrix} \tag{18}$$

By solving eqn (14), the displacements at the junctions can be obtained and then the whole displacement field can finally be obtained (Liu and Achenbach, 1994b).

3.4. *A technique for determining the horizontal crack*

The ultimate goal of the analytical modeling is to find out the relationship between the characteristics of cracks in the plate and the responses of the plate to the imposed loads. A technique to find out the relationship is to move the loading along the surface of the plate [change the value of d in eqn (2)], and in the meantime pick up the resulting displacement in the z-direction at the central point of the distributed load ($x = d$), then plot the responses of the plate while the load scans over the plate. For a plate without crack, the scanning result is a horizontal line, because the responses of the uncracked plate at the central point of load are independent of the location of the load, as infinitely long plates are considered in this paper. However, for a cracked plate, the scanning result will no longer be a constant, and the responses can be expected to have a significant change when the load passes over the crack tips. This provides a way to find out the length of the crack in the plate. Moreover, the responses in the region in between the two crack tips can be expected to contain information related to the thickness of domain III (see Fig. 1) and the crack depth. By investigating these responses, the depth of the crack can also be found. The following section will show how this technique works by numerical experiments.

4. NUMERICAL EXPERIMENTS

Numerical experiments are made for a homogeneous isotropic plate with a Poisson's ratio of $\mu = 1/3$ and a hybrid laminated plate denoted by $[C90/G45/G-45]_s$ with horizontal cracks. In the notation for the laminate, the letters C and G stand, respectively, for carbon/epoxy and glass/epoxy layers, while the numbers following the letters indicate the

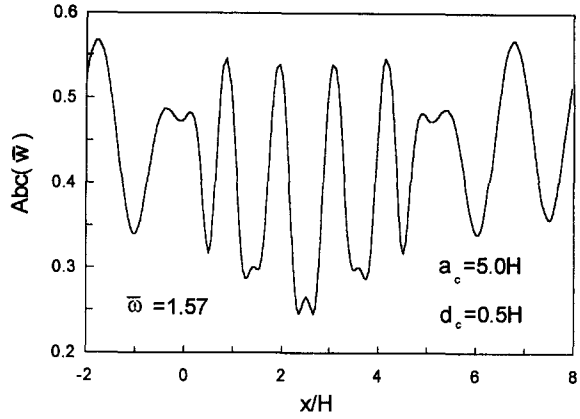

Fig. 2. Scanning results of the absolute value of the vertical displacement amplitude for an isotropic plate ($\mu = 1/3$) with a horizontal crack. The left crack tip of the crack is at the origin.

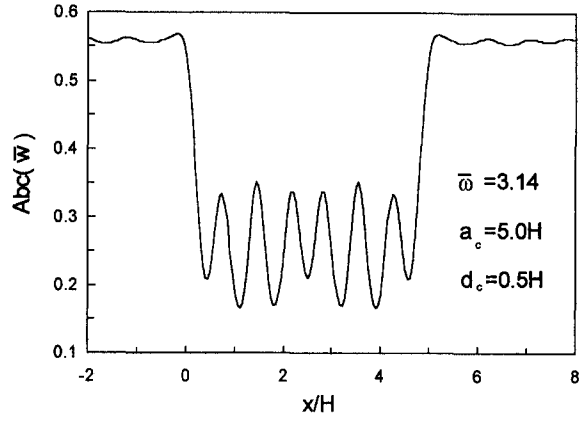

Fig. 3. As in Fig. 2, but the dimensionless frequency of the load is 3.14.

angle of the fiber orientation with respect to the x-axis and the subscript s indicates that the plate is symmetrically stacked. Material constants of carbon/epoxy and glass/epoxy can be found in a paper by Liu *et al.* (1991a).

In this paper the following dimensionless parameters are used:

$$\bar{x} = x/H, \quad \bar{w} = c_{44}w/q_0, \quad \bar{\omega} = \omega H/c_s$$
$$c_s = \sqrt{c_{44}/\rho}, \quad c_{44} = \mathbf{c}(4,4), \quad \bar{d}_c = d_c/H, \tag{19}$$

where w is the displacement in the z-direction, and $\mathbf{c}$, ρ and c_s are the material constants matrix, density and shear wave velocity of the reference material, respectively. For the homogeneous isotropic plate, the reference material is the material of the plate. For the $[C90/G45/G-45]_s$ plate, C90 is chosen as the reference material.

4.1. *Detection of a crack in an isotropic plate*

4.1.1. *Crack length.* The responses of the plate to the harmonic load are dependent on the frequencies of the load. The frequency dependency of the scanning result of a cracked plate is first investigated. Figures 2–4 show the scanning results of the absolute value of displacement amplitude of the plate excited by the load as given by eqn (1). The results are obtained by using SEM, and the frequencies of the load are $1.57\bar{\omega}$ (Fig. 2), $3.14\bar{\omega}$ (Fig. 3) and $6.28\bar{\omega}$ (Fig. 4), whose corresponding shear wavelengths are $4.0H$, $2.0H$ and $1.0H$, respectively. From Figs 2–4 it is noted that the crack length can be approximately determined from the pattern change of the results when the load passes over the crack, and that the frequency of $3.14\bar{\omega}$ is the best to determine the crack length because the results in

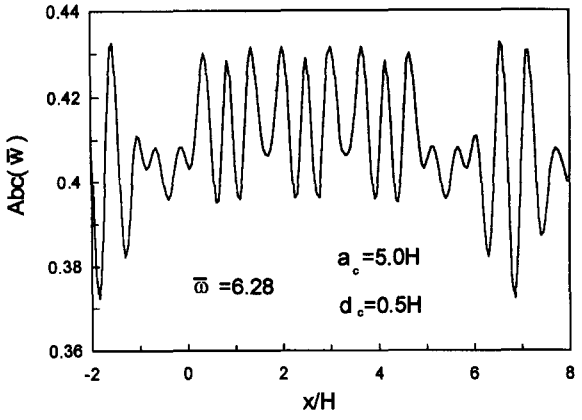

Fig. 4. As in Fig. 2, but the dimensionless frequency of the load is 6.28.

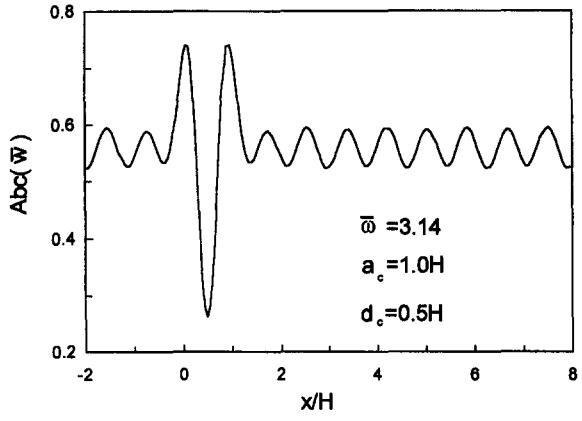

Fig. 5. Scanning results of the absolute value of the vertical displacement amplitude for an isotropic plate ($\mu = 1/3$) with a horizontal crack. The left crack tip of the crack is at the origin.

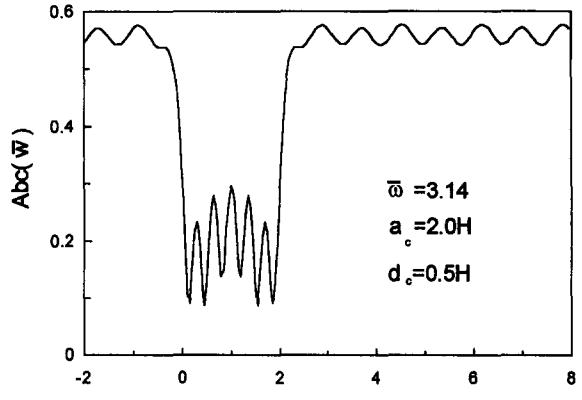

Fig. 6. As in Fig. 5, but the crack length is $2.0H$.

between the two crack tips are significantly different from the results in the uncracked region. Hence the following results are obtained by using a harmonic load with a frequency of $3.14\bar{\omega}$.

Scanning results for other crack lengths, $a_c = 1.0H$, $2.0H$ and $3.0H$, are shown in Figs 5–7. In all the cases, the positions of the cracks can be determined approximately from the scanning result. Although the exact crack length is difficult to find out from the scanning result, clear images of the cracks can be obtained.

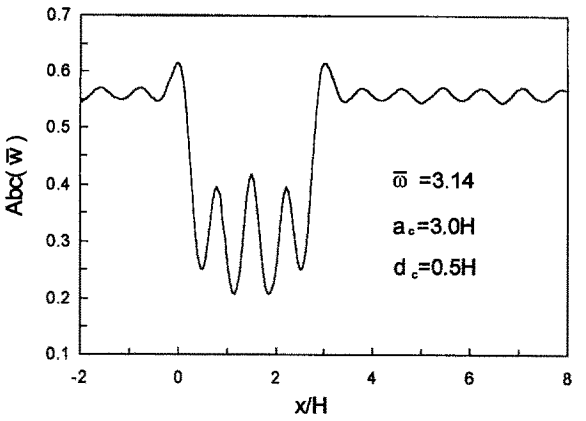

Fig. 7. As in Fig. 5, but the crack length is $3.0H$.

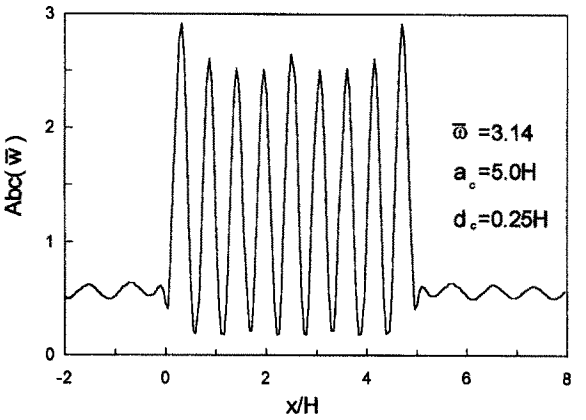

Fig. 8. As in Fig. 3, but the crack depth is $0.25H$.

4.1.2. *Depth of the crack.* From Fig. 3 an important fact can be observed. The spacings of the peaks of the oscillations in the region of $0 < x < a_c$ are about the same. Comparing with Figs 3 and 7, it is found that the spacings of the peaks of the oscillations in $0 < x < a_c$ for $a_c = 3.0H$ are almost the same as for $a_c = 5.0H$. This fact tells us that the peak spacing of the oscillation is less dependent on the crack length.

Changing the depth of the crack to $0.25H$ for the case of $a_c = 5.0H$, the scanning results are shown in Fig. 8. It is found again that the peak spacings of the oscillation in the region of $0 < x < a_c$ are almost the same. However, the peak spacing for the $d_c = 0.25H$ (Fig. 8) is much smaller than for $d_c = 0.5H$ (Fig. 3). This is a very important fact because it indicates that the depth of the crack is related to the peak spacing of the oscillations in the region of $0 < x < a_c$.

To find out the relationship between the crack depth and the peak spacing of the oscillations, we investigated the scanning results of the plate using the following steps.

1. Calculate the scanning results for plates with various crack depths and lengths, and output the results over the region of $0 < x < a_c$.
2. Transfer the results to wave number domain

$$\tilde{w}(k) = \int_0^{a_c} \bar{w}(x) \exp(-ikx)\, dx, \tag{20}$$

where the k is the wave number. The spectra of the results are shown in Figs 9–12. It is noted that the wave number, at which the response has the maximum value, is related to the peak spacings of the oscillation in $0 < x < a_c$. In this paper, we call

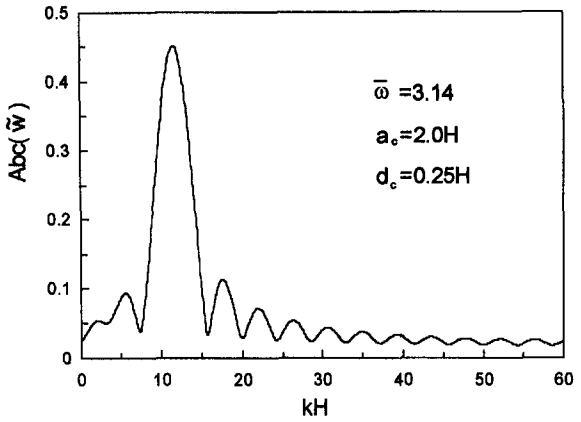

Fig. 9. Spectrum of scanning results for an isotropic plate ($\mu = 1/3$) with a horizontal crack.

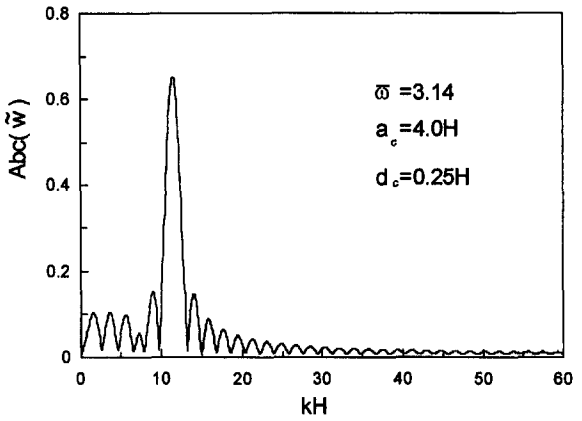

Fig. 10. As in Fig. 9, but the crack length is $4.0H$.

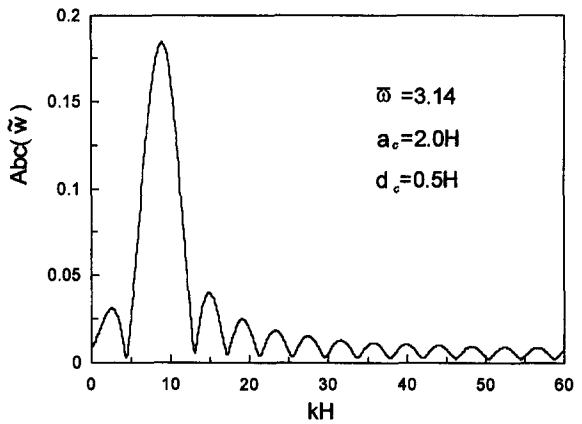

Fig. 11. As in Fig. 9, but the crack depth is $0.5H$.

this wave number the central wave number, and denote it by k_{max}. By comparing Figs 9–12, it can be found that the central wave numbers are almost the same for the same crack depths (Figs 9 and 10; Figs 11 and 12), and are significantly different for the different crack depths (Figs 9 and 11; Figs 10 and 12).

3. Select the central wave numbers k_{max}, and plot them against the crack depths d_c. The final results are shown in Fig. 13.

From Fig. 13, the crack depth is easily found from the central wave number of the scanning results. It is also noted that the $k_{max} - d_c$ curves are less dependent on the crack length for

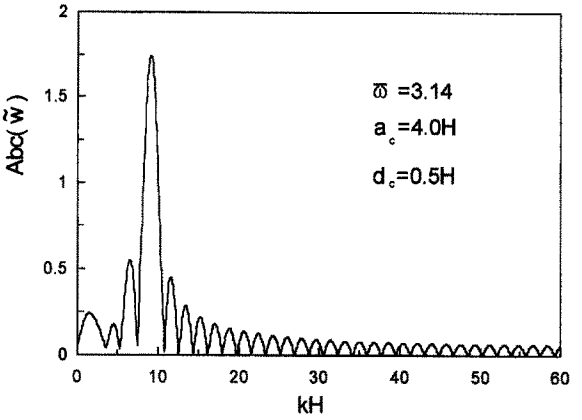

Fig. 12. As in Fig. 10, but the crack depth is $0.5H$.

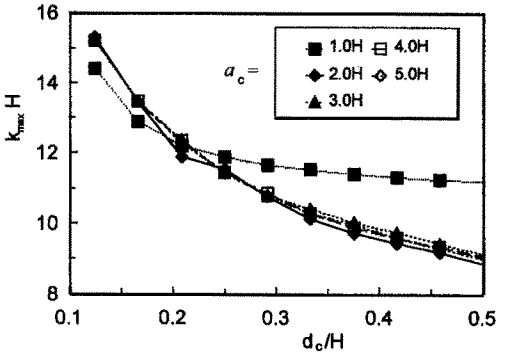

Fig. 13. Depth dependency of the central wave number on the depth of the crack for an isotropic plate ($\mu = 1/3$).

the case of $a_c \geqslant 2.0H$. Hence the crack depth can be obtained quite accurately even though the crack length can only be obtained approximately by the method described in Section 4.1.1. Using polynomial regression of degree 3, the relationship between the crack depth and the central wave number can be obtained as follows:

$$\bar{d}_c = 5.0279 - 0.97988p + 0.067041p^2 - 0.0015653p^3, \tag{21}$$

where $p = k_{max}H$. Equation (21) is valid for $8.86 \leqslant p \leqslant 15.3$, $0.125H \leqslant d_c \leqslant 0.5H$, $2.0H \leqslant a_c \leqslant 5.0H$. The reason to limit the usage of eqn (21) is that the samples for obtaining it have been taken in these regions. To expand the usage of eqn (21), further investigation has to be made. We have used this equation to predict the crack depth of a cracked plate with crack length of $10.0H$ and crack depth of $0.25H$ by the following procedure. First, the scanning results in the region of $0.0 < x < a_c$ are computed for the cracked plate with crack length of $10.0H$ and crack depth of $0.25H$. The results in the wave number domain are then calculated using eqn (20) and the central wave number obtained to be $11.3343/H$. Finally, the predicted depth from eqn (21) is $0.2478H$, compared to $0.25H$ as given. Obviously, this is a very good prediction.

4.2. *Detection of a crack in an anisotropic laminated plate*

4.2.1. *Crack length.* Figures 14 and 15 show the scanning results of a hybrid laminated plate $[C90/G+45/G-45]_s$ for crack lengths of $2.0H$ and $4.0H$. Clear images of crack length in the plates can be obtained.

4.2.2. *Depth of the crack.* Following the same procedure described in Section 4.1.2, the $k_{max} - d_c$ curves for the $[C90/G+45/G-45]_s$ plate can be obtained and are shown in Fig. 16.

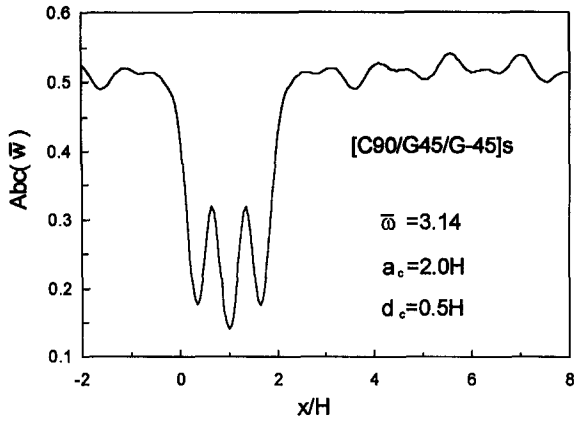

Fig. 14. Scanning results of the absolute value of the vertical displacement amplitude for an anisotropic laminated plate with a horizontal crack. The left crack tip of the crack is at the origin.

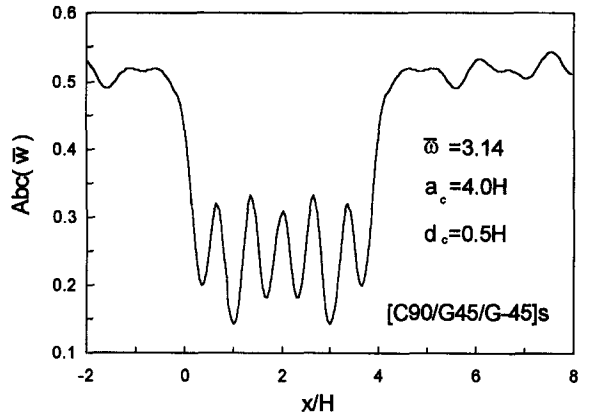

Fig. 15. As in Fig. 14, but the crack length is $4.0H$.

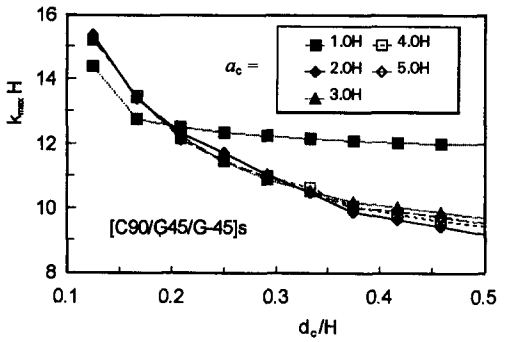

Fig. 16. Depth dependency of the central wave number on the depth of the crack for a hybrid laminated plate.

Using polynomial regression of degree 3, a formulation of the relationship between the crack depth and the central wave number can be obtained as follows:

$$\bar{d}_c = 6.1914 - 1.2144p + 0.082547p^2 - 0.0019016p^3, \tag{22}$$

where $p = k_{max}H$. Equation (22) is valid for $9.19 < p < 15.4$, $0.125H < d_c < 0.5H$, $2.0H < a_c < 5.0H$.

5. COMMENTS ON THE PROPOSED TECHNIQUE

Conventional ultrasonic techniques, such as B- and C-scan techniques, are widely used in non-destructive testing and are effective in detecting cracks and flaws that are parallel to the surfaces of the plates. For the cases discussed in Section 4, crack lengths and depths can be accurately obtained by these techniques. However, these techniques are difficult to use for vertically and obliquely situated cracks and flaws with an oblique or curved surface. Moreover, the efficiency of these techniques depends on the surface quality of the crack and the flaw. The reason is that these techniques are using pulses of body waves such as longitudinal, and are based on the measurement of reflected or transmitted pulses in the real time. For a vertical or oblique crack or a crack with very poor quality of reflection or a flaw with an oblique or curved surface, the signals may not come back, and hence it is difficult to characterize this kind of crack and flaw. In the technique presented in this paper, time-harmonic input loads are used. Cracks have been characterized from the pattern of responses of the plate to the time-harmonic input at a single frequency. These responses consist of a number of guided waves scattered by cracks and are less dependent on the quality of the crack surface but heavily dependent on the size, orientation and location of the cracks. Therefore, the present technique has the potential to detect vertical and oblique cracks, cracks of poor surface quality and flaws with oblique or curved surfaces. In this paper, only horizontal cracks are discussed. Detection of flaws will be discussed in a follow-up paper and oblique cracks will also be considered in the near future.

The disadvantage of the present technique is that it is difficult to obtain a very accurate crack length especially for short cracks. For a crack of $a_c < 2.0H$, eqns (21) and (22) cannot be used, and the crack depth has to be determined by using its k_{max}–d_c curve for a given crack length.

6. CONCLUSIONS

A technique for the characterization of a horizontal crack in anisotropic laminated plates has been presented. Numerical experiments have been made by using the strip element method. It has been shown that the technique presented can be used successfully to detect both the length and the depth of horizontal cracks in anisotropic laminated plates. This technique is expected to be used in practical problems, such as in the characterizations of delaminations in composite laminated plates.

Acknowledgement—When the first author was working at Northwestern University, U.S.A., he had many discussions with Professor J. D. Achenbach about some of this work. The authors are very grateful to Professor Achenbach for his helpful discussions and suggestions. The first author's work while at Northwestern University was supported by Grant N00014-89-J-1362/P.9 from the Offfice of Naval Research.

REFERENCES

Al-Nassar, Y. N., Datta, S. K. and Shah, A. H. (1991). Scattering of Lamb waves by a normal rectangular strip weldment. *Ultrasonics* **29,** 125–132.

Datta, S. K., Ju, T. H. and Shah, A. H. (1992). Scattering of an impact wave by a crack in a composite plate. *ASME J. Appl. Mech.* **59,** 596–603.

Karim, M. R., Awal, M. A. and Kundu, T. (1992). Elastic wave scattering by cracks and inclusions in plates: in-plane case. *Int. J. Solids Structures* **29**(19), 2355–2367.

Karunasena, W. M., Shah, A. H. and Datta, S. K. (1991). Plane-strain-wave scattering by cracks in laminated composite plates. *ASCE J. Engng Mech.* **117**(8), 1738–1754.

Liu, G. R. and Achenbach, J. D. (1994a). A strip element method for stress analysis of anisotropic linearly elastic solids. *ASME J. Appl. Mech.* In press.

Liu, G. R. and Achenbach, J. D. (1994b). SEM method to analyse scattering by cracks in anisotropic laminated plates. *ASME J. Appl. Mech.* In press.

Liu, G. R., Tani, J., Ohyoshi, T. and Watanabe, K. (1991a). Characteristic wave surfaces in anisotropic laminated plates. *ASME J. Vibr. Acoustics* **113,** 230–239.

Liu, S. W., Datta, S. K. and Ju, T. H. (1991b). Transient scattering of Rayleigh Lamb waves by a surface-breaking crack: comparison of numerical simulation and experiment. *J. Nondestruc. Eval.* **10**(3), 111–126.

Liu, S. W. and Datta, S. K. (1993). Scattering of ultrasonic waves by cracks in a plate. *ASME J. Appl. Mech.* **60,** 352–357.

Von Estorff, O., Pais, A. L. and Kausel, E. (1990). Some observations on time domain and frequency domain boundary elements. *Int. J. Numer. Meth. Engng* **29,** 785–800.

Xu, P. C. and Mal, A. K. (1987). Calculation of the inplane Green's functions for a layered viscoelastic solid. *Bull. Seismological Soc. America* **77**(5), 1823–1837.